

Research Article

GREEN SYNTHESIS AND CHARACTERIZATION OF ISOLATED FLAVONOID MEDIATED COPPER NANOPARTICLES BY USING *THESPESIA POPULNEA* LEAF EXTRACT AND ITS EVALUATION OF ANTI-OXIDANT AND ANTI-CANCER ACTIVITY

MARIMUTHU GOKUL*^a, UMARANI G. ^a, AYYAMPERUMAL ESAKKI^b

^aMadurai Medical College, Madurai, Tamilnadu, India 625020, ^bMadras Medical College, Chennai, Tamilnadu, India 600003
Email: gokulvengatnov25@gmail.com

Received: 27 Sep 2021 Revised and Accepted: 10 Dec 2021

ABSTRACT

Objective: An Eco-friendly process of Green Synthesis of Copper Nano-particles (CuNPs) is an important aspect in the field of Nanotechnology using alternative feedstock, energy minimization, the design of less toxic and inherently safer chemicals.

Methods: In this study, Copper Nano-Particles were synthesized by using isolated flavonoids to induce the reduction of Cu²⁺ ions to CuNPs and also act as a capping and stabilizing agent. The solutions of CuSO₄ and flavonoid were used as stock solutions for the preparation of CuNPs. Aqueous flavonoid (Quercetin) solution was mixed with CuSO₄ solution separately. The reaction mixtures were immediately placed in a hot plate magnetic stirrer at 2000 rpm, 50-60 °C temperature and observed the change in colour of the solution from colourless to coloured solution. The synthesized CuNPs were characterized by various spectral methods for structural analysis of Nano-particles and *In vitro* and *In vivo* evaluation for anti-cancer activity.

Results: The results described that the Copper Nano-particles are crystalline and amorphous with an average size of 295.4 nm and highly stable and having good hydrogen peroxide scavenging effect, reducing power and total antioxidant activity with the IC₅₀ value of 59.24 µg/ml, 24.35 µg/ml and 16.83 µg/ml respectively. The *in vitro* (HepG2 and MCF-7 cell lines) anti-cancer activity showing good results with IC₅₀ values of 57.56 µg/ml for HepG2 cell line and 56.41 µg/ml for MCF-7 cell line. The *in vivo* anti-cancer activity also showing good results.

Conclusion: Thus, this method can be used for rapid and eco-friendly biosynthesis of stable and active Copper Nano-particles.

Keywords: Antioxidant(s), Apoptosis, Cancer, Nanoparticle(s), Particle size, Spectroscopy, X-ray powder diffraction (XRD)

© 2022 The Authors. Published by Innovare Academic Sciences Pvt Ltd. This is an open-access article under the CC BY license (<http://creativecommons.org/licenses/by/4.0/>)
DOI: <http://dx.doi.org/10.22159/ijcr.2022v6i1.197>. Journal homepage: <https://ijcr.info/index.php/journal>

INTRODUCTION

Nanotechnology is an enabling technology which deals with nano-meter-sized tiny objects. It is predicted that nanotechnology will be developed at various levels: materials, devices and systems. The nanomaterials level is the leading at present, both in scientific knowledge and in commercial applications [1-6].

Nano herbal drug delivery systems have a dormant future for increasing the activity and minimizing the problems associated by medicinal plants. So, the herbal nano-carriers help to treat threatening diseases like cancer, Diabetes etc. The herbal drugs can be utilized in a greater form with increased efficacy by putting together into modern dosage forms. This can be attained by designing novel drug delivery systems for herbal constituents [7].

Metal nanomaterials are known to have vast applications in the field of agriculture, energy, environment, and medicine. Metal nanomaterials are hugely biocompatible and have various pharmacological activities. Interestingly, plant-based 'Green' synthesis of nanomaterials has drawn great attention due to its cost-effective, eco-friendly, non-pathogenic, rapid, and also efficiency in the treatment process. In addition, Green synthesis provides a single-step technique as well as trouble-free to scale up for large synthesis [8-12].

The plant-based Metal Nano-particles (MNPs) showed excellent anti-microbial, anti-cancer, anti-diabetic, anti-inflammatory, antioxidant, and immuno-modulatory activities. Most of the previous reports authenticate that the presence of phytochemicals including alkaloids, flavonoids, phenols, terpenoids, alcohols, sugars and proteins in the plant materials are involved in the reduction and stabilization of metal ions. Although the synthesis of MNPs using a single active substance from plant extract will be helpful for the purification of nanoparticles, and further study on such MNPs in the biomedical sector is needed to treat specific diseases. Recent reports highlighted the fact that flavonoids widely existing in the plant extract contributing a major role in the bio-reduction of metal ionic into nanoparticle formation [13-20].

Cancer is a general term applied to a series of malignant diseases which may affects many different parts of the body. These diseases are characterized by rapid and uncontrolled formation of abnormal cells, which may mass together to form a growth or tumour, or proliferate throughout the body. Cancer is the most common cause of death throughout the world and is accountable for an estimated 9.6 million deaths in 2018. Across many countries, about 1 in 6 deaths is due to cancer. Cancer is basically a disease of cells characterized by the loss of normal cellular growth, maturation and multiplication, and thus homeostasis is disturbed [21-23].

Copper Nanoparticles are acts as Anti-cancer agent involving the process that, 1. Accumulation of CuNPs on the cell surface from pits which causes cell leakage, 2. DNA damage due to the interaction with CuNPs, 3. Interaction of Cu ions with sulphydral group of proteins, 4. Entry of CuNPs and Cu ions inside the cell develops oxidative stress, which leads to cell death, 5. Interaction of CuNPs with cell membrane decreases the transmembrane electrochemical potential, which effects membrane integrity.

The aim of the study is to synthesize, Characterise and Biological evaluation of Copper Nano Particles in which the followings are involved.

MATERIALS AND METHODS

All the chemical reagents used in this experiment were analytical grade purchased from Lobachemie, Chennai, Tamilnadu, India. The *Thespesia populnea* leaves were collected at 10 °20'02.0"N 79 °11'37.8"E Kalathur, Pattukkottai(Tk), Thanjavur(Dt), Tamilnadu, India on 19.08.2018 and was authenticated by Dr. Stephen, Professor, Department of Botany, American college, Madurai-625 020 on 20.08.2018. The leaves were collected and shade dried. It was powdered and the coarse powder was sieved and stored in a well-closed container.

Green synthesis of copper nanoparticles by using flavonoid quercetin as a stabilizing agent

Double distilled water has been used throughout the synthesis process. 1 mmol solutions of CuSO₄ and 0.02% flavonoid were used as stock solutions for the preparation of CuNPs. The flavonoid (Quercetin) was dissolved in water by slightly increasing the pH using NaOH as they are sparingly soluble in water. After complete dissolution of flavonoid, the pH was neutralized using HCl. 10 ml of aqueous flavonoid (Quercetin) solution was mixed with 90 ml of 1 mmol CuSO₄ solution separately. The reaction mixtures were immediately placed in a hot plate magnetic stirrer at 2000 rpm, at 50-60 °C temperature and observed for change in colour of the solution. After 60 min, the resulting solution was turned out from light green to dark brown colour indicating the formation of copper nanoparticles. After the incubation, the solution was centrifuged at 12,000 rpm for 25 min. The pellet was resuspended in distilled water and stored in the freezer for further study [24-26].

Characterization of synthesized CuNPs

UV-visible spectrum

UV-visible absorbance spectroscopy has been proved to be a significant technique for the detection of synthesized metallic NPs because the peak position and shape of the spectra are sensitive to the particle size. The reduction of pure Cu to Copper Nanoparticle was observed by measuring the UV-Vis spectrum, the most confirmatory tool for the detection of Surface Plasmon Resonance property (SPR) of CuNPs. UV-Vis spectral analysis was done by using a UV-Vis spectrophotometer (SHIMADZU) at a range 400 to 700 nm [27-31].

FT-IR spectrophotometer

The characterization of functional groups at the surface of Cu nanoparticles by flavonoid(Quercetin) were investigated by FTIR analysis and the spectra were scanned in the range of 4000–450 cm⁻¹. The sample was prepared by dispersing the CuNPs uniformly in a matrix of dry KBr, compressed to form an almost transparent disc. This technique is used to acquire an infrared spectrum of absorption, emission, photoconductivity or Raman scattering of a solid, liquid and gas [27-31].

Atomic absorption spectrometry

Atomic Absorption Spectroscopy (AAS) is a technique of quantitative determination of chemical elements by using the absorption of optical radiations by free atoms in the gaseous state. The metal content was determined by flame atomic absorption spectroscopy equipped with a hollow cathode lamp and an air-acetylene flame (Analytik Jena AG, nova A 350, Jena, Germany). The wavelengths (nm) used for the determination of the various metals were: Copper 324.8, Nickel 232.0, Cadmium 228.8 and Lead 283.3. Gas flow was 15 (L/min) and Element: Cu Atomizer/Gas Flow Rate: Setup Fuel Gas Flow Rate (L/min): 1.8, Support Gas Flow Rate (L/min): 15.0 [27-31].

Particle size distribution and polydispersity index

Average particle size, particle size distribution and Polydispersity index were measured by MALVERN ZETASIZER instrument. Stability and particle size distribution were measured by standard values such as,

- D (0.9) corresponds to particle size immediately above 90% of the sample
- D (0.5) corresponds to particle size immediately above 50% of the sample
- D (0.1) corresponds to particle size immediately above 10% of the sample.

ZETA potential

Zeta potential is an electrical potential which is exhibited by any particulate matter in suspension. If all the particles within the suspension having large zeta potential values (positive or negative) they have a tendency to repel one another and there will be no tendency for the particles to come together. However, if the particles have low zeta potential values, then there will be no force to prevent the particles to come together and being flocculated.

The zeta potential value can be related to the stability of colloidal system. A value of +25 mV to -25 mV can be taken as an arbitrary value that separates low charged surface from a high charged surface. Zeta potential was analyzed by MALVERN ZETASIZER instrument [27-31].

X-ray diffraction (XRD)

The CuNPs solution was centrifuged, re-dispersed with distilled water and lyophilized to obtain pure CuNPs and CuNPs Pellets. The XRD analysis was done with X-ray diffractometer at a scanning speed of 0.15 ° per min from 10-100 ° (2θ degree). XRD pattern is characterized by the interplanar d-spacing and the relative intensities (I/I₀) of the strongest peaks in the pattern under the Hanawalt system. It was acknowledged the position of values of product crystallinity or amorphous nature [27-31].

Scanning electron microscopy (SEM)

Scanning Electron Microscope using a focused beam of electrons, it generates various signals at the surface of a solid sample which reveals the details of surface morphology, chemical composition, crystalline structure and therefore, the orientation of materials constituting the sample. For visualizing FMCuNPs under SEM 10 μl was uniformly spread on a glass slide and allowed to dry at room temperature. After gold coating the sample with a Polaron E5100 gold sputter coater, the morphology was observed under a Philips 505 electron microscope at an accelerating voltage of 20 kV. SEM image of flavonoid (Quercetin) mediated biosynthesized copper nanoparticles indicated the formation of homogeneous and relative capping of spherical CuNPs [27-31].

Energy-dispersive X-ray spectroscopy (EDXS)

Energy Dispersive X-ray Spectroscopy (EDXS) is a semi-quantitative X-ray micro-analytical technique that can come up with information about the elemental composition of a sample. It is useful in identifying metals and certain kinds of polymeric materials with distinctive elemental signatures. During EDXS Analysis, an electron beam is scanned over the surface of the sample and therefore the electrons strike and stimulates the sample.

Almost instantaneously, as each element returns to its original energy level, it emits X-rays of specific energies and at different wavelengths characteristic of the element [27-31].

Swiss target prediction of isolated quercetin

Swiss Target Prediction is based on the study that indistinguishable bioactive molecules are more probably to share similar targets. It is an online server to exactly predict the targets of bioactive molecules based on a mixture of 2D and 3D similarity measures with known ligands [32].

Pharmacological evaluations of synthesized FMCuNPs

Anti-oxidant activity

The Anti-oxidant activity of FMCuNPs was performed by the following methods,

Determination of scavenging activity against hydrogen peroxide

The test was done with the help of UV-Vis Spectrophotometer Shimadzu (Model 1800). To 1 ml of test solutions of different concentrations, 3.8 ml of 0.1 M phosphate buffer solution (pH 7.4) and then 0.2 ml of hydrogen peroxide solution were added. The absorbance of the reaction mixture was measured at 230 nm after 10 min. The reaction mixture without the sample was used as blank and Ascorbic acid was used as standard. The percentage inhibition of hydrogen peroxide was calculated applying the formula,

$$\% \text{ inhibition} = \frac{[(\text{Control}-\text{Test})/\text{Control}] \times 100}{}$$

The concentration of the sample required for 50 % reduction in absorbance (IC₅₀) was calculated using linear regression analysis [33-35].

Determination of reducing power assay

The reducing power ability of CuNPs was screened by assessing the ability of the test extract to reduce FeCl₃ solution as mentioned by Oyaizu *et al.*, (1986). 0.1 to 0.5 ml of sample solution (1 mg/ml) was mixed with 0.75 ml of phosphate buffer and 0.75 ml of 1 % Potassium Ferricyanide [K₃Fe(CN)₆] and incubated at 50 °C for 20 min. About 0.75 ml of 10 % Trichloroacetic acid was added to the mixture and allowed to stand for 10 min. The whole mixture was then centrifuged at 3000 rpm for 10 min. Finally, 1.5 ml of the supernatant was removed and mixed with 1.5 ml of distilled water and 0.1 ml of 0.1% Ferric Chloride solution and the absorbance was measured at 700 nm in UV-Visible Spectrophotometer. Ascorbic acid solution was used as standard and phosphate buffer solution was used as blank solution [33-35].

Determination of total antioxidant activity

The total antioxidant activity of the CuNPs was evaluated by Phospho molybdenum method using UV-Visible spectrophotometer, Shimadzu (Model) 1800. An aliquot of 0.3 ml of various concentrations of the sample was treated with 2.7 ml of the reagent H₂SO₄, sodium orthophosphate and ammonium molybdate). Just in case of blank, 0.3 ml of methanol was utilized in place of the sample. The sample tubes were incubated in a boiling water bath at 95 °C for about 90 min. The samples were adjusted to room temperature by cooling; the absorbance of each and every concentration of the aqueous solution was measured at 695 nm against blank. Similarly, Vitamin C standard was treated. The antioxidant activity was expressed as an equivalent of vitamin C (µg/ml) [33-35].

In vitro anticancer activity

MTT assay by using liver cancer cell line (HepG5) and breast cancer cell line (MCF-7)

The MTT (3-(4, 5-dimethylthiazolyl)-2, 5-diphenyltetrazolium bromide) assay, based on the conversion of the yellow Tetrazolium salt-MTT, to purple-Formazan crystals by metabolically active cells, provides a quantitative determination of viable cells. HepG5, MCF-7 Cells are plated on to 96 well plates at a cell density of 2×10⁵ ml⁻¹ per well in 100µL of RPMI 1640 and allowed to grow in CO₂ incubator for 24 h (37°C, 5% CO₂). Then the medium is replaced by a fresh medium containing various concentrations of samples (FMCuNP's) for 24 h. The cells are incubated for 24-48 h (37°C, 5% CO₂). Then, 20 µL MTT stock solution (0.5 mg/ml) was added to each well and incubated for 4 h. The medium is removed and 200 µL DMSO (Dimethyl Sulfoxide) is added to each well to dissolve the MTT metabolic product. Then the plate is shaken at 150 rpm for 5 min and the optical density is measured at 570 nm. Untreated cells (basal) are used as a control of viability (100%) and the results are expressed as % viability (log) relative to the control [36-38].

$$\text{Cytotoxicity (\%)} = \frac{[(A-B)/A] \times 100}{}$$

Where,

A = Absorbance of the untreated group

B = Absorbance of treated group

In vivo anticancer activity

In the present work, cell lines induced cancer in mice was used to evaluate the anticancer activity. Swiss albino mice and Dalton's Lymphoma Ascites (DLA) cell was approved and supplied by Research Advisory Council and Institutional Animal Ethical Committee, Amala Cancer Research Center, Trissur, Kerala, India. The cells were maintained alive in Swiss albino mice by intraperitoneal transplantation. While transferring the tumour cells to the grouped animal, the DLA cells were aspirated from the greater peritoneal sac of the mice using saline. The cell counts were done and further dilution were made in such a manner that total cells should be 1 x 10⁶, this dilution was given intraperitoneally. Let the tumour grow within the mice for minimum of seven days before starting treatments [35-42].

Treatment protocol

Swiss Albino mice were divided in to four groups of six each. All the animals in three groups were injected with DLA cells (1 x 10⁶ cells per mouse) intraperitoneally, and the remaining one group is the normal control group.

Group 1 served as the normal control.

Group 2 served as the tumour control. Group 1 and group 2 received normal diet and Water.

Group 3 served as the positive control, was treated with Fluorouracil (inj.) at 20 mg/kg body weight, Intraperitoneal.

Group 4 served as a treatment control group and received Quercetin mediated Copper nanoparticles of at a dose of 10 mg/kg through intraperitoneally.

Treatment

In this current study, drug treatment was given once daily for 14 d after 24 h of inoculation. On 14th day, after the last dose, all mice from every group were sacrificed and the blood was withdrawn from each mouse by retro-orbital plexus method and the following parameters were checked.

Evaluation of clinical parameters

1) Haematological parameters

i) WBC count

The total WBC count was found to be increased in cancer control when compared with normal and treated tumor-bearing mice. The total WBC counts were found to decrease significantly in animals treated with extract when compared with cancer control, indicating that the anti-tumour nature of the extract.

ii) RBC count

RBC count decreases with tumour bearing mice when compared with Normal control mice.

iii) Platelet count

In Hodgkin lymphoma, increased in platelet count is often reported in laboratory findings.

iv) Haemoglobin count

Haemoglobin count decreases with tumour bearing mice when compared with Normal control mice.

iv) Packed cell volume

In any case of anaemia the packed cell volume decreases.

2) Serum enzyme and lipid profile

i) Total cholesterol and triglyceride (lipid profile)

Abnormal blood lipid profile has been correlated with cancer. In Hodgkin lymphoma, high level of cholesterol and low level of triglyceride has been reported.

ii) Liver enzymes (AST, ALT, ALP)

Abnormal liver function noticed in a patient with Hodgkin lymphoma, that these liver enzyme levels markedly increases in tumor bearing mice. ALP is an enzyme mostly derived from the liver, bones and in lesser amount from the intestines, placenta, kidneys and leukocytes. An increase in ALP levels in the serum is normally associated with various diseases. ALP is composed of a group of enzyme that catalyzes the phosphate esters in an alkaline environment, generating an organic radical and inorganic phosphate. Notably elevated serum ALP, hyper alkaline-phosphataemia, is seen primarily with more specific disorders; including malignant biliary cirrhosis, hepatic lymphoma and sarcoidosis.

3) Derived parameters

1. Bodyweight

All the mice were weighed from the starting day to 15th day of the study. Average increase in weight of the body on the 15th day was determined.

2. Percentage increase in life span (ILS)

% ILS was calculated by means of the formula,

$$\% \text{ILS} = (\text{Lifespan of treated group} / \text{lifespan of the control group}) - 1 \times 100$$

- All biochemical investigations were carried out by using COBAS MIRA PLUS-S Auto analyzer from Roche Switzerland.
- Hematological tests were executed in COBAS MICROS OT 18 from Roche Switzerland.

3. Cancer cell count

About 0.1 ml of fluid was withdrawn from the peritoneal sac of each and every mouse with the help of sterile syringe. The fluid was diluted with 0.8 ml of ice-cold normal saline or sterile Phosphate Buffer solution and 0.1 ml of Trypan blue (0.1 mg/ml). The total numbers of the living cells were counted using haemocytometer.

$$\text{Cell count} = \text{No of cells Dilution} / (\text{Area} \times \text{Thickness of liquid film})$$

Effect of FMCuNPs on survival time

Animals were divided into four groups; six animals each in a group. Except the normal control group, the remaining groups were inoculated with DLA cells (1x10⁶ cells/mouse) intraperitoneally on day '0' and treatment with FMCuNPs started 24 h after inoculation, at a dose of 200 mg/kg/day. The normal and tumor control group was treated with the same volume of 0.9% Sodium Chloride solution. All the treatments were given to animals for the duration of 14 d. The increase in life span (ILS) of each groups of 6 mice was noted. The anti-tumor efficacy of FMCuNPs was compared with that of 5-Fluorouracil (Dabur pharmaceutical ltd. India; 5-FU, 20 mg/kg/day, i. p for 14 d). The ILS of the drug-treated groups was compared with that of the control group using the following formula:

$$\text{Increase in lifespan} = [(T-C)/C] \times 100$$

Where T = number of days that the treated animal survived.

C = number of days that the control animals survived.

RESULTS AND DISCUSSION

Green synthesis of nanoparticles using plants as bio-reductants have more advantages than other biological processes because here no need to maintain the cell culture and also suitable for large scale synthesis.

Green synthesis of flavonoid mediated Cu nanoparticles with *thespesia populnea* (L.) leaf extract

Quercetin, a plant flavonoid found in fruits, vegetables and grains which is reported to have an inflammatory and antioxidant property. It is also beneficial in the treatment of allergy and blood pressure. In this present study, we have isolated the Quercetin from the aqueous extract of *Thespesia populnea* leaves. The active Quercetin was used as a reactant to nucleate nanoparticles in solution. Initially, the confirmation of the formation of CuNPs was done through monitoring the change in colour of the reaction mixture with concomitant UV-Visible spectroscopy. Addition of optimal volume of CuSO_4 has changed the colour of the solution from light green to dark brown colour validating the formation of CuNPs (fig. 1).



Fig. 1: Observation of color changes during synthesis of copper nanoparticles at different time

The Flavonoid, Quercetin which can reduce metal ions to metal NPs shown in fig. 2.



Fig. 2: Flavonoid quercetin responsible for the bio-reduction of metal ions

The possible equation for the synthesis of CuNPs is mentioned in fig. 3.

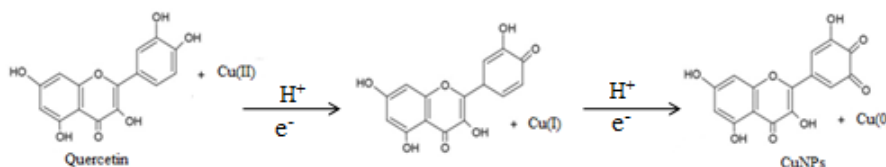


Fig. 3: Synthetic reaction process for flavonoid mediated copper nanoparticles

UV-Vis spectrophotometry

Next the synthesized Copper nanoparticles (CuNPs) were characterized by UV-Vis spectroscopy. The UV-Visible spectrum of the CuNPs solution was recorded at different time intervals (1, 3, 6, 12 and 24 h) (fig. 4). The appearance of a sharp and high peak at 620 nm in the spectrum indicates the

stability and size of the Copper nanoparticles. Enhanced absorbance implies the reduction of Cu^{++} to Cu as the formation of nanoparticles results in concomitant accumulation of CuNPs.

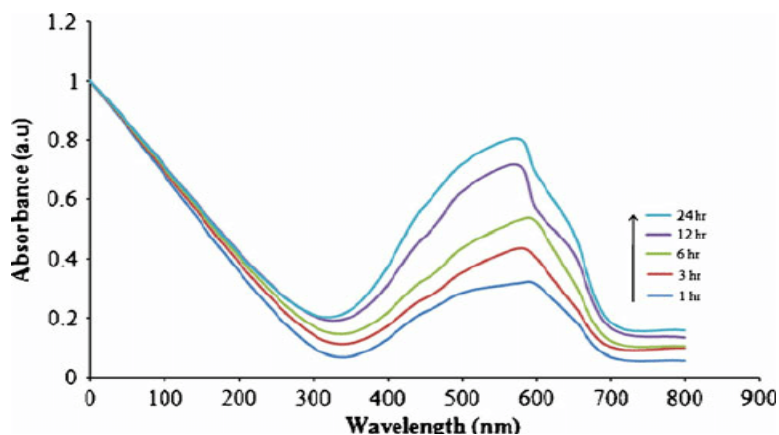


Fig. 4: UV-visible spectrum of FMCuNPs at different time interval during the synthetic process

IR-spectrum of FMCuNPs

After confirming the formation of Copper nanoparticles, we assayed their stability by FTIR spectra of bio-reduced CuNPs (fig. 5). Major peaks at 3338.78 cm^{-1} (O-H stretching of phenolic group), 1618.28 cm^{-1} (C=O stretching), and 1095.57 cm^{-1} (C-O-C stretching), were detected suggesting the presence of Quercetin in CuNPs.

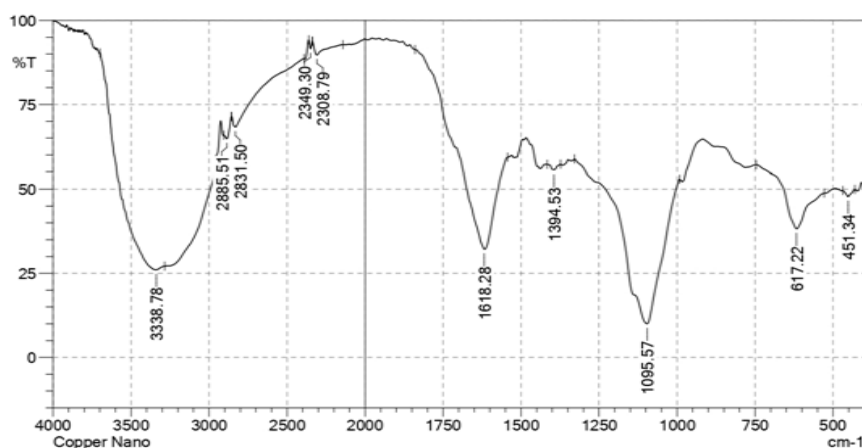


Fig. 5: FTIR spectra of synthesized CuNPs

Atomic absorption spectroscopy

Next, we have analysed the sample by atomic absorption spectroscopy at 320 nm. The absorbance of Copper nanoparticles present in the sample was (fig. 7) compared with the standard calibration graph (fig. 6). Comparative data reveals that the tested sample has the same concentration as that of standard one and it lies within the permissible range (10 ppm). It also obeys the Beer-Lambert's laws.

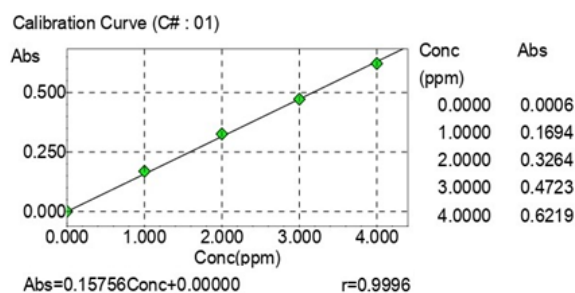


Fig. 6: Calibration curve of copper

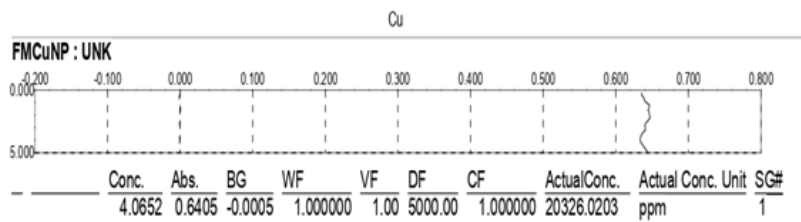


Fig. 7: Atomic absorption spectrum of FMCuNPs

Particle size distribution and polydispersity index

We have verified the identity of the synthesized nanoparticles by measuring the particle size and polydispersity index of the sample by DLS study. Our data shows that the zeta potential, polydispersity index and particle size of FMCuNPs are 23.5, 0.213 and 295.4 nm, respectively (fig. 8). Hence we can decipher that FMCuNPs are nano-sized particles and stable in manner.

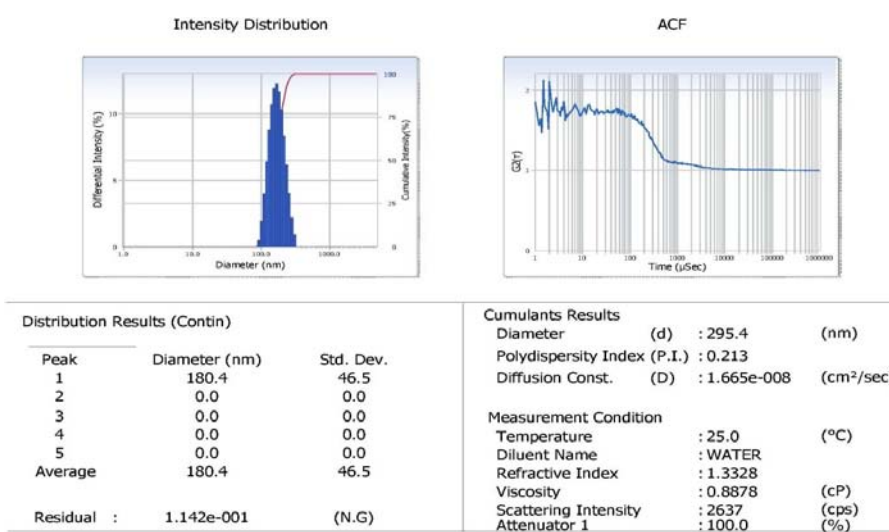


Fig. 8: Particle size and polydispersity index of FMCuNPs

Zeta potential analysis

Further to elucidate the surface property of the synthesized nanoparticles, we have performed Zeta Potential Analysis. Zeta Potential of the synthesized nanoparticles was found to lie within the desired millivolt range (-30mV to +30mV). The higher charge on the surface of FMCuNPs acts as a repulsive force between the FMCuNPs which made them stable and devoid of agglomeration (fig. 9). Thus, Zeta Potential Analysis has reconfirmed the stability of the synthesised FMCuNPs.

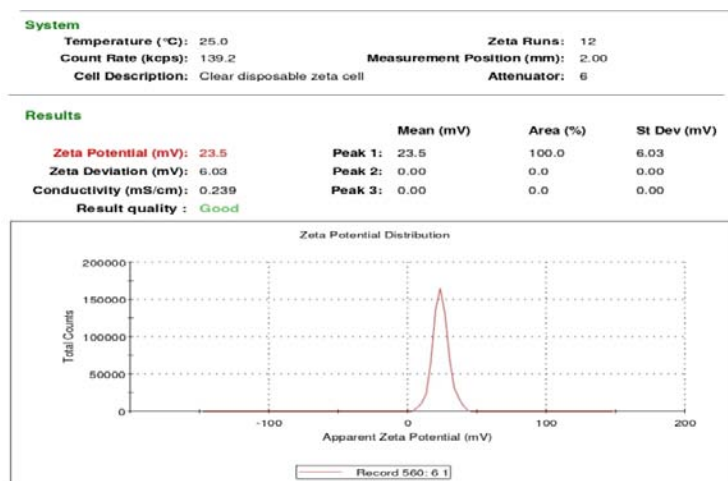


Fig. 9: Zeta potential graph of FMCuNPs

X-ray diffraction analysis of FMCuNPs

Next, XRD analysis of FMCuNPs has been done to quantify the relative occurrence of the crystalline and amorphous structured species in the nanoparticle sample. Fig. 10 depicts a typical XRD profile of synthesized FMCuNPs with diffraction peaks at 2θ of 25.38° , 26.57° , 15.3° , 31.49° , and 18.6° are representatives of (1 1 0), (1 1 2), (2 0 2), (1 1 3) and (3 7 4) planes respectively. The diffraction peaks are well synchronized with JCPDS Card (Joint Committee on Powder Diffraction Standards, 89-2529) and thus, we can interpret that 20.3% of the green synthesized FMCuNPs are present in crystalline nature and the remaining 79.7% have acquired an amorphous appearance. The calculated average crystallite size of green synthesized FMCuNPs was found to be in the range of 20-100 nm.

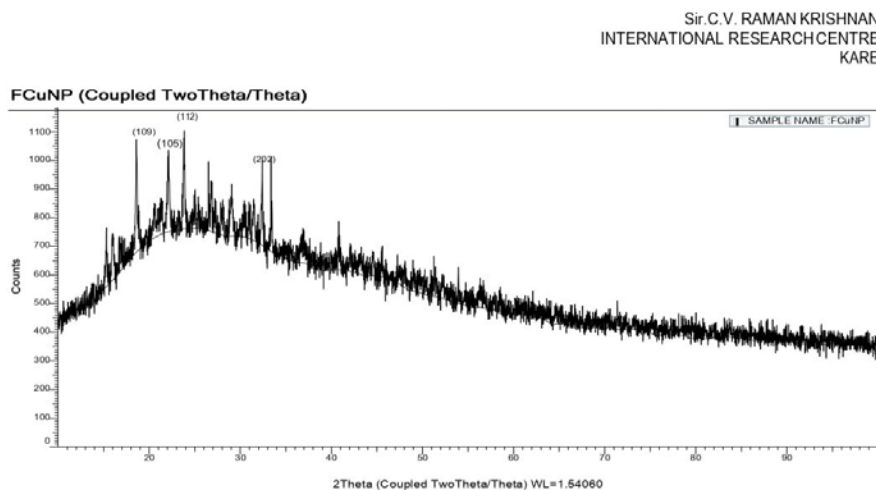


Fig. 10: X-ray diffraction spectrum of green synthesized FMCuNPs

Scanning electron microscopy (SEM) analysis

The morphological characteristics of green synthesized FMCuNPs were examined by Field Emission Gun-Scanning Electron Microscopy (FE-SEM). Fig. 11 displays the electro micrograph of the green synthesised FMCuNPs depicting their morphology features. FMCuNPs appears like agglomerated spherical shaped entity and are dispersed as clusters. The size of particles is considerably small and falls in the range of 20-300 nm, further strengthening the data obtained from the XRD spectrum (fig. 10).

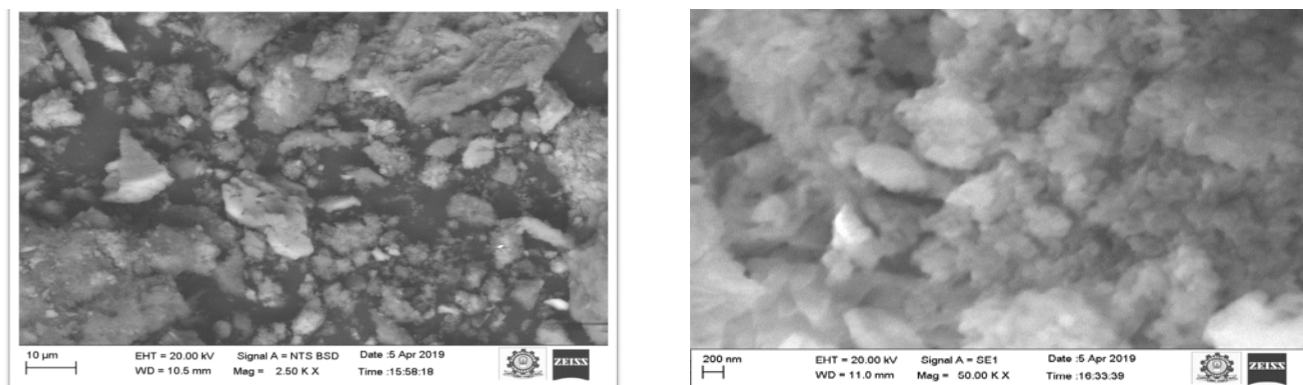


Fig. 11: SEM image of green synthesized FMCuNPs at 10 nm and 200 nm in size range

Energy-dispersive X-ray spectroscopy (EDAX)

The chemical composition of green synthesized FMCuNPs has been studied by the EDAX analysis (Fig.12). Our data has revealed the chemical composition of green synthesized nanoparticles containing the elements in atomic percent 12.6% of Cu, 46.0% of C and 41.8% O. EDAX results confirmed that green synthesized FMCuNPs are uncontaminated pure materials containing only copper and flavonoid related atoms.

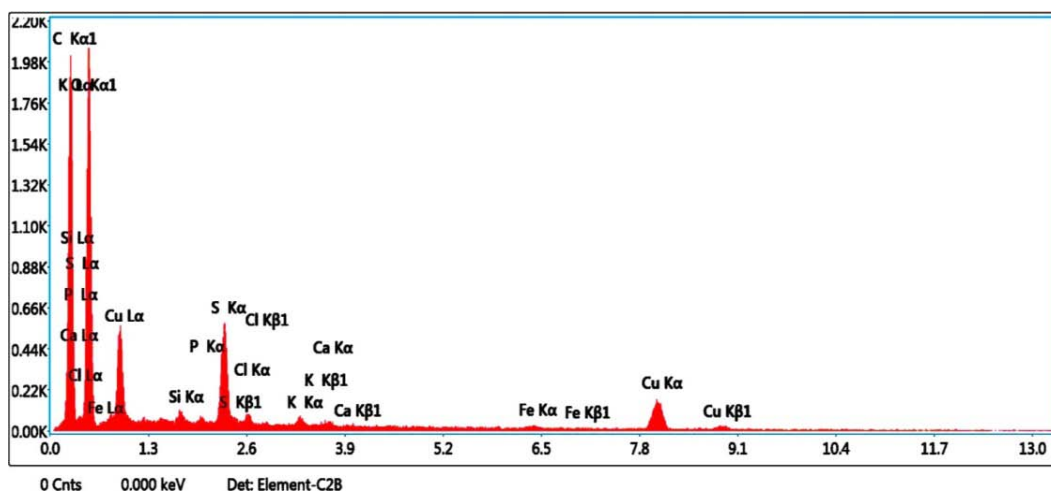


Fig. 12: EDAX spectrum of green synthesized FMCuNPs

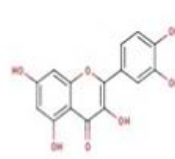
Swiss target prediction of isolated quercetin structure

Next, we have used the “Swiss target prediction,” an online tool for exploring the probable macromolecular target of our synthesized nanoparticles. This analysis has verified that the isolated Quercetin may have affinity against various cellular receptors. According to the Swiss Target Prediction report of Quercetin (fig. 13), receptors associated with cellular proliferation and potential redox maintenance like epidermal growth factor receptor, Tyrosine kinase receptor are probable primary target of Quercetin.

SwissTargetPrediction report:

Reference:
Goller D., Michielin O. & Zoete V.
Shaping the interaction landscape of bioactive molecules. *Bioinformatics* (2013) 29:3073-3079.

Query Molecule



Target	Uniprot ID	Gene code	ChEMBL ID	Probability	# sim. cmpds (3D / 2D)	Target Class
Carbonic anhydrase 12	O43570	CA12	CHEMBL3242	<div style="width: 100%; height: 10px; background-color: green;"></div>	3 / 5	Enzyme
Epidermal growth factor receptor	P00533	EGFR	CHEMBL203	<div style="width: 100%; height: 10px; background-color: green;"></div>	6 / 28	Tyr Kinase
Carbonic anhydrase 1	P00915	CA1	CHEMBL261	<div style="width: 100%; height: 10px; background-color: green;"></div>	10 / 7	Enzyme
Carbonic anhydrase 2	P00918	CA2	CHEMBL205	<div style="width: 100%; height: 10px; background-color: green;"></div>	10 / 7	Enzyme
Phospholipase A2	P04054	PLA2G1B	CHEMBL4426	<div style="width: 100%; height: 10px; background-color: green;"></div>	1 / 1	Enzyme
Receptor tyrosine-protein kinase erbB-2 (by homology)	P04626	ERBB2	CHEMBL1824	<div style="width: 100%; height: 10px; background-color: green;"></div>	6 / 28	Tyr Kinase
Myeloperoxidase	P05164	MPO	CHEMBL2439	<div style="width: 100%; height: 10px; background-color: green;"></div>	1 / 1	Enzyme
Cytochrome P450 1A2 (by homology)	P05177	CYP1A2	CHEMBL3356	<div style="width: 100%; height: 10px; background-color: green;"></div>	8 / 13	Enzyme
Cyclin-dependent kinase 1	P06493	CDK1	CHEMBL308	<div style="width: 100%; height: 10px; background-color: green;"></div>	3 / 27	Ser_Thr Kinase
Carbonic anhydrase 3	P07451	CA3	CHEMBL2885	<div style="width: 100%; height: 10px; background-color: green;"></div>	10 / 7	Enzyme
Alpha-trypsin chain 1	P07477	PRSS1	CHEMBL209	<div style="width: 100%; height: 10px; background-color: green;"></div>	1 / 2	Serine Protease
PEX	P08253	MMP2	CHEMBL333	<div style="width: 100%; height: 10px; background-color: green;"></div>	5 / 2	Metallo Protease
Stromelysin-1	P08254	MMP3	CHEMBL283	<div style="width: 100%; height: 10px; background-color: green;"></div>	3 / 2	Metallo Protease
Arachidonate 5-lipoxygenase	P09917	ALOX5	CHEMBL215	<div style="width: 100%; height: 10px; background-color: green;"></div>	10 / 52	Enzyme
Microtubule-associated protein tau	P10636	MAPT	CHEMBL1293224	<div style="width: 100%; height: 10px; background-color: green;"></div>	25 / 77	Unclassified

Fig. 12: Swiss target prediction of isolated quercetin

Pharmacological evaluations of synthesized FMCuNPs

In order to assay the anti-cancerous potential of the FMCuNPs, we have furthered our study by subjecting the green synthesized FMCuNPs to *In vitro* anti-oxidant studies. It includes hydrogen peroxide scavenging activity, total antioxidant capacity and reducing power assay.

Determination of hydrogen peroxide scavenging activity of greenly synthesized FMCuNPs

The inhibitory concentration (IC₅₀) for the hydrogen peroxide scavenging effect of greenly synthesized FMCuNPs (fig. 14 and table 1) is found to be 59.24µg/ml whereas ascorbic acid a potent standard antioxidant exhibit the IC₅₀ value to be 60.15µg/ml.

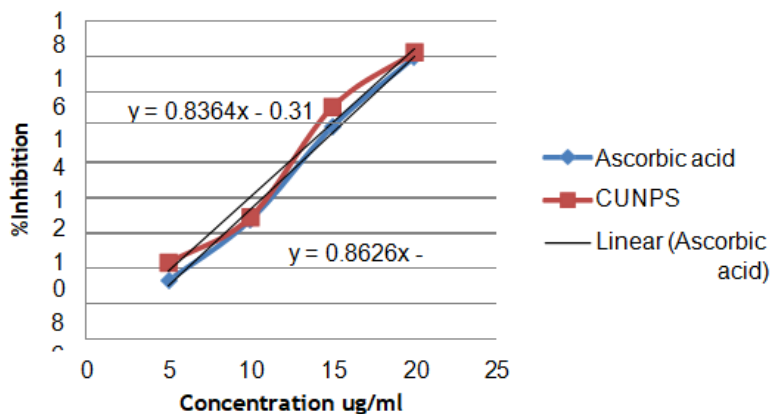


Fig. 14: Hydrogen peroxide scavenging effect by ascorbic acid

Table 1: Determination of hydrogen peroxide scavenging activity of greenly synthesized FMCuNPs

S. No.	Concentration of ascorbic acid (µg/ml)	Percentage inhibition of ascorbic acid standard (µg/ml)	Concentration of greenly synthesized FMCuNPs(µg/ml)	Percentage inhibition greenly synthesized FMCuNPs (µg/ml)
1	5	3.32	5	4.34
2	10	6.75	10	6.91
3	15	12.02	15	13.12
4	20	15.94	20	16.21
	IC ₅₀	60.15	IC ₅₀	59.24

Determination of reducing power assay of greenly synthesized FMCuNPs

The inhibitory concentration (IC₅₀) for the reducing power assay of greenly synthesized FMCuNPs (fig. 15 and table 2) is found to be 24.35µg/ml, comparable to Ascorbic acid, having IC₅₀ value of 22.98µg/ml.

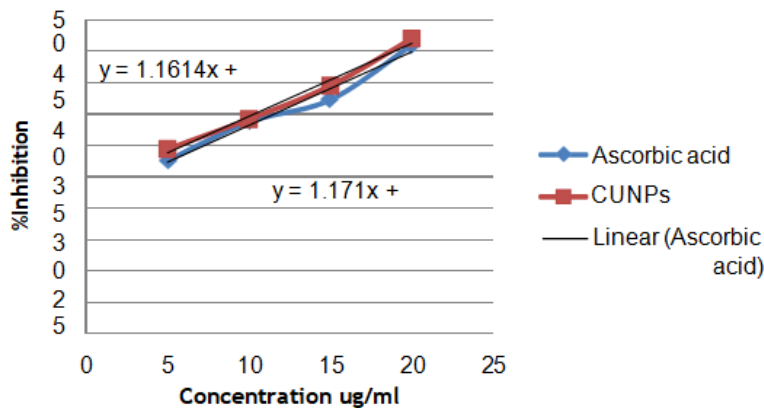


Fig. 15: Reducing power assay by ascorbic acid

Table 2: Determination of reducing power assay of greenly synthesized FMCuNPs

S. No.	Concentration of ascorbic acid ($\mu\text{g/ml}$)	Percentage inhibition of ascorbic acid standard ($\mu\text{g/ml}$)	Concentration of greenly synthesized FMCuNPs ($\mu\text{g/ml}$)	Percentage inhibition greenly synthesized FMCuNPs ($\mu\text{g/ml}$)
1	5	27.61	5	29.43
2	10	33.74	10	34.21
3	15	37.27	15	39.54
4	20	45.95	20	47.01
	IC ₅₀	22.98	IC ₅₀	24.35

Determination of total antioxidant assay of greenly synthesized FMCuNPs

Moreover, the designed nanomaterial was found to have significant antioxidant potential. The inhibitory concentration (IC₅₀) for the total antioxidant assay of green synthesized FMCuNPs (fig. 16 and table 3) is found to be 16.83 $\mu\text{g/ml}$.

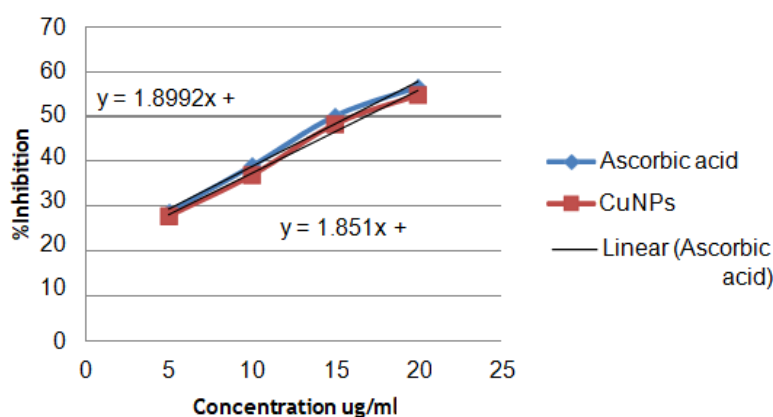


Fig. 16: Total anti-oxidant effect by ascorbic acid

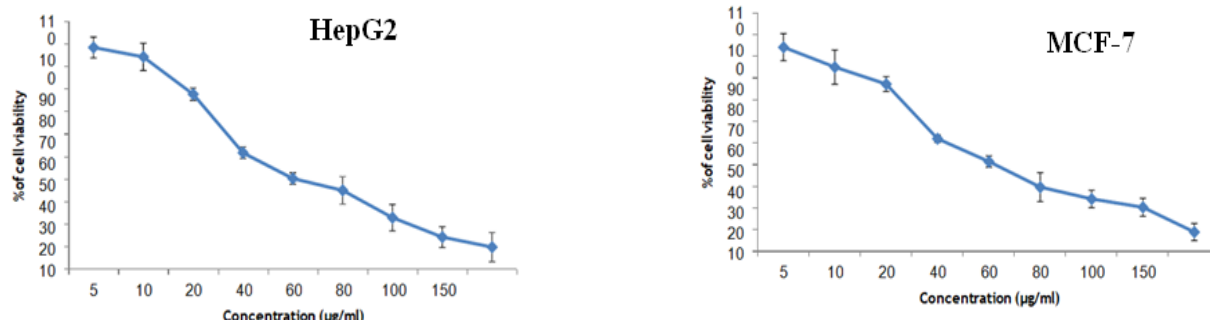
Table 3: Determination of total antioxidant assay of greenly synthesized FMCuNPs

S. No.	Concentration of ascorbic acid ($\mu\text{g/ml}$)	Percentage inhibition of ascorbic acid standard ($\mu\text{g/ml}$)	Concentration of greenly synthesized FMCuNPs ($\mu\text{g/ml}$)	Percentage inhibition greenly synthesized FMCuNPs ($\mu\text{g/ml}$)
1	5	28.67	5	27.81
2	10	38.97	10	36.94
3	15	50.11	15	48.31
4	20	56.61	20	54.87
	IC ₅₀	23.29	IC ₅₀	16.83

In vitro anticancer activity

MTT assay of green synthesized FMCuNPs using liver cancer cell line (HepG2) and breast cancer (MCF-7) cell line

Finally, to analyse the cytotoxic activity of the Green synthesized FMCuNPs, we performed MTT assay with two well-established cancerous cell line HepG2 and MCF-7. The greenly synthesized FMCuNPs had IC₅₀ values of 57.56 $\mu\text{g/ml}$ for HepG2 cell line and 56.41 $\mu\text{g/ml}$ for MCF-7 cell line (fig. 17 and table 4). The comparative study of morphology alteration of the cell line in response to the treatment with FMCuNPs is also depicted in fig. 18. Thus our data showed that FMCuNPs has exerted a promising and selective cytotoxic activity against both HepG2 and MCF-7 cell line.



n=3, mean±sd

Fig. 17: Cytotoxicity of FMCuNPs on HepG2 and MCF-7 cells

Table 4: Percentage inhibition of different concentrations of greenly synthesized FMCuNPs on HepG2 and MCF-7 Cells

Compound	Cell line	Concentration (µg/ml)	% Viability	IC ₅₀ (µg/ml)
Greenly Synthesized FMCuNPs	Liver Cancer Cell Line (HepG2 Cell)	5	98.6524	57.56
		10	94.4745	
		20	77.8977	
		40	51.8869	
		60	40.4313	
		80	35.1752	
		100	23.0459	
		150	14.4205	
		200	9.9730	
			Breast cancer Cell line (MCF-7 cell)	
10	84.8258			
20	76.9900			
40	51.7412			
60	41.1693			
80	29.3532			
100	23.8806			
150	20.0248			
200	8.5820			
Compound	Cell Line			Control

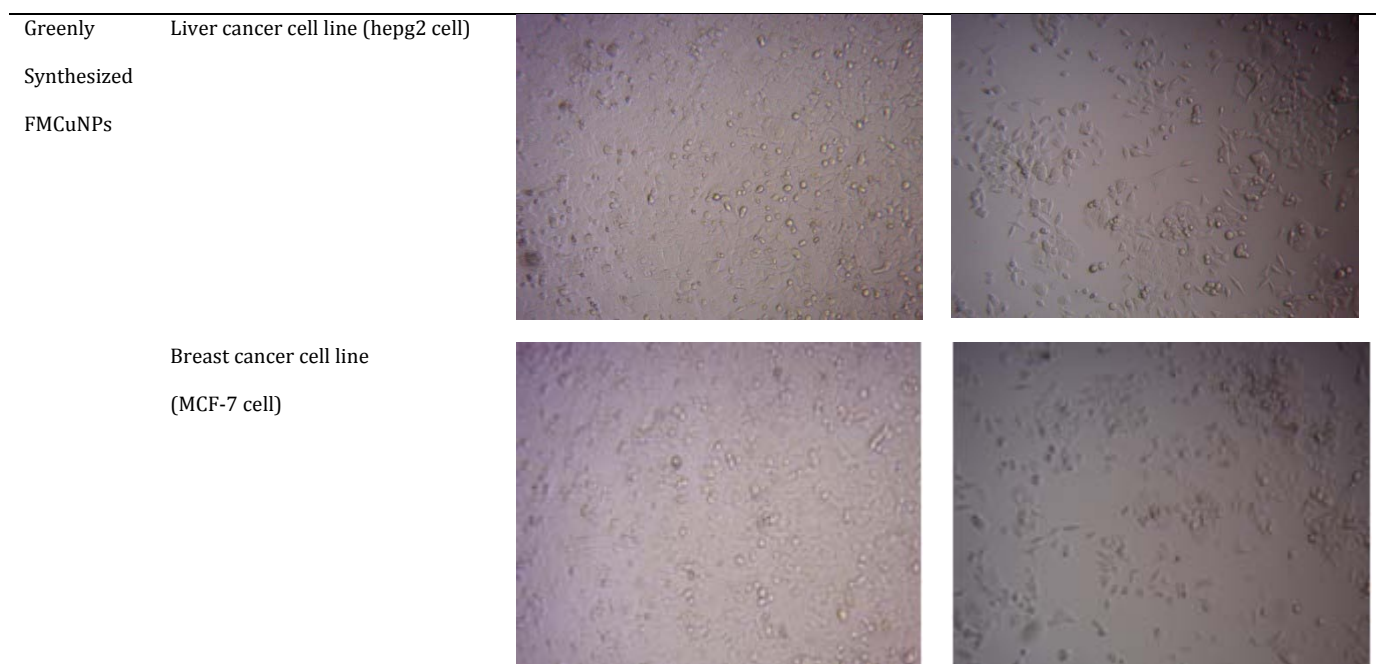


Fig. 18: Morphological changes in HepG2 and MCF-7 Cell lines

***In vivo* anticancer activity of greenly synthesized FMCuNPs by using dalton's lymphoma ascites in mice**

Next, to validate our observation in *in vivo* model we have introduced cell line-induced mice cancer model in this study. Dalton's Lymphoma Ascites (1×10^6) was injected intraperitoneally to mice and the mice were kept for 7 d to allow the significant growth of tumour mass. Next, a group of these mice were treated with FMCuNPs intraperitoneally and a group were treated with fluorouracil and marked as the positive control. After completion of all the treatment, the mice were sacrificed; the blood was withdrawn from each mouse by retro-orbital plexus method and several clinical parameters like haematological parameter, serum enzyme and lipid profile etc were assayed.

Effect on haematological parameters

Analysis of haematological parameters reveals a significant decrease of RBC, Haemoglobin (Hb), platelets and a notable increase of WBC in the DLA control group compared to the normal control group (table 5). On the contrary, treatment with FMCuNPs at the dose of 200 mg/kg significantly increases the Hb content, RBC, platelets with simultaneous reduction of the WBC count in comparison to DLA control group. Thus our data validates the anticancer potential of the FMCuNPs.

Table 5: Effect of FMCuNPs on hematological parameters

Treatment	Total WBC cells/mlx10 ³	RBC count mill/mm ³	Hb Gm/dl	PCV %	Platelets Lakhs/mm ³
G1	9.95±1.28	4.27±0.99	12.40±2.42	14.65±2.84	3.20±0.78
G2	14.15±2.65 ^{a**}	2.32±0.48 ^{a**}	7.32±0.8	31.45±3.55 ^{a**}	1.60±0.62 ^{a**}
G3	11.35±1.92 ^{b**}	3.95±0.85 ^{b**}	11.4±1.80 ^{b**}	19.21±2.60 ^{b**}	2.67±0.54 ^{b**}
G4	12.40±2.32 ^{b*}	3.30±0.82 ^{b*}	10.80±1.78 ^{b*}	22.24±1.60 ^{b*}	2.32±0.74 ^{b*}

G1–Normal Control, G2–Cancer Control, G3–Positive control, G4–Treatment control of FMCUNPs-Flavonoid Mediated Copper Nanoparticles, All values are expressed as mean±SEM for 6 animals in each group, ^a–Values are significantly different from Normal control (G1) at P<0.001, ^b–Values are significantly different from cancer control (G2) at P<0.01, ^{**}–Values are significantly different from cancer control (G2) at P<0.001

Effect on biochemical parameters

The introduction of DLA cells results in a significant increase of the level of Total Cholesterol, Aspartate aminotransferase, Alanine aminotransferase, Alkaline phosphatase in the tumour control animals (G2), when compared to the normal group. Surprisingly, the treatment with FMCuNPs at the dose of 200 mg/kg body weight reversed these changes towards the normal level (table 6). The biochemical parameter of the FMCuNPs treated set is found to be comparable with that of the normal group.

Table 6: Effect of FMCuNPs on serum enzymes and lipid proteins

Treatment	Cholesterol (mg/dl)	TGL (mg/dl)	AST (U/l)	ALT (U/l)	ALP (U/l)
G ₁	96.30±3.65	125.4±4.50	34.44±1.30	32.40±1.32	128.35±2.30
G ₂	142.95±4.60 ^{a**}	204.45±6.40 ^{a**}	6.45±2.80 ^{a**}	56.20±2.25 ^{a**}	240.50±4.28 ^{a**}
G ₃	110.50±3.92 ^{b**}	150.55±3.80 ^{b**}	54.25±1.80 ^{b**}	42.40±1.70 ^{b**}	165.30±2.40 ^{b**}
G ₄	122.30±2.55 ^{b*}	163.22±2.40 ^{b*}	72.40±1.92 ^{b*}	45.50±1.25 ^{b*}	188.65±2.65 ^{b*}

G₁–Normal Control, G₂–Cancer Control, G₃–Positive control, G₄–Treatment control of FMCUNPs-Flavonoid Mediated Copper Nanoparticles, All values are expressed as mean±SEM for 6 animals in each group, ^a–Values are significantly different from Normal control (G₁) at P<0.001, ^b–Values are significantly different from cancer control (G₂) at P<0.01, ^{**}–Values are significantly different from cancer control (G₂) at P<0.001

Effect on tumour growth

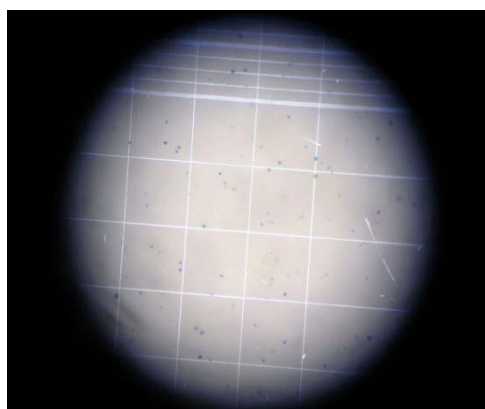
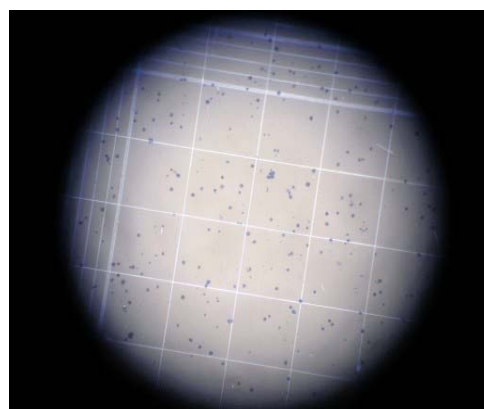
Next we asked whether FMCuNPs has any effect on the survival of animal having cancerous growth. In the DLA tumour control group, the average life span of animals was reduced to 50%, whereas FMCuNPs at the dose of 200 mg/kg body weight increases the life span to 70% and 72%, respectively. Thus our data reveals that the FMCuNPs has a considerable potential of augmentation of life span of animals having cancerous growth. The anti-tumor nature of FMCuNPs was further verified by the significant reduction in percent increase of body weight of animals treated with FMCuNPs at the dose of 200 mg/kg body weight when compared to DLA tumor-bearing mice. It was also supported by the significant reduction in packed cell volume and viable tumour cell count in both the extent of treatment when compared to the DLA tumour control (table 7).

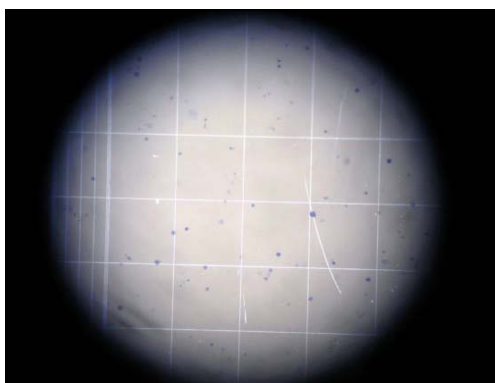
Table 7: Effect of FMCuNPs on the life span, body weight and cancer cell count of tumor-induced mice

Treatment	Number of animals	% ILS life span	Increase in body weight grams	Cancer cell count ml X 10 ⁶
G ₁	6	>30 d	2.20±0.50	-
G ₂	6	50%	7.84±1.10 ^{a**}	2.60±0.32 ^{a**}
G ₃	6	92%	3.72±0.55 ^{b**}	1.39±0.31 ^{b**}
G ₄	6	72%	6.13±0.90 ^{b*}	1.98±0.40 ^{b*}

G₁–Normal Control, G₂–Cancer Control, G₃–Positive control, G₄–Treatment control of FMCUNPs-Flavonoid Mediated Copper Nanoparticles, All values are expressed as mean±SEM for 6 animals in each group, ^a–Values are significantly different from Normal control (G₁) at P<0.001, ^b–Values are significantly different from cancer control (G₂) at P<0.01, ^{**}–Values are significantly different from cancer control (G₂) at P<0.001

Viable cell count (fig. 19)

**Normal control****Cancer control**



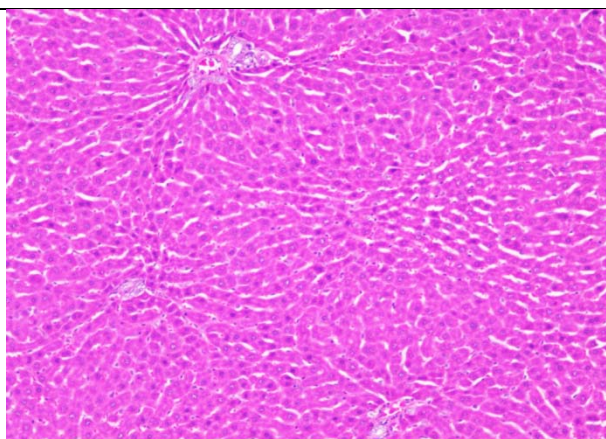
Positive control



Treatment control-FMCuNPs

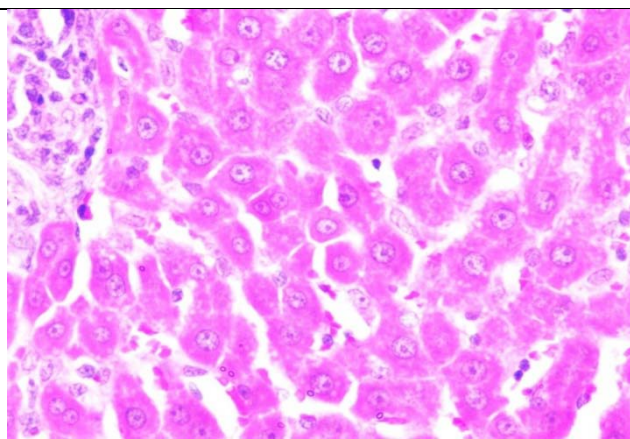
Fig. 19: Viable cell count of *in vivo* anticancer activity of FMCuNPs

Histopathological results (Animal liver) (fig. 20)



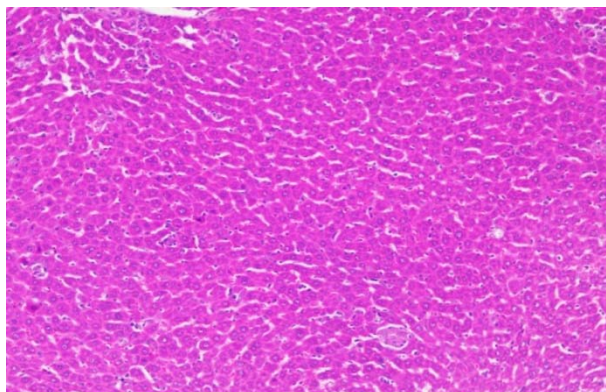
Normal control

Section show structure of liver with sheets of hepatocytes separated by sinusoids cartial vein and portal tract appear normal



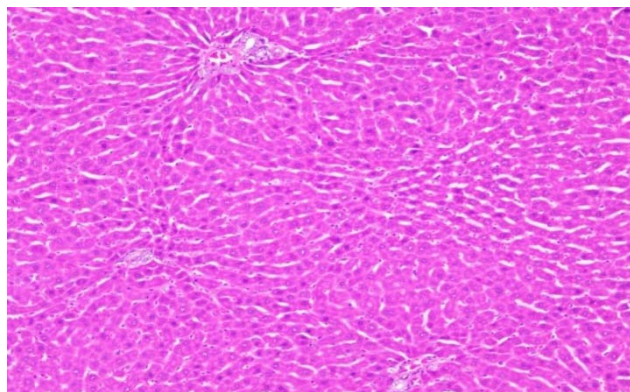
Cancer control

Section shows the structure of liver presented hepatic congestion at sinusoids and the portal vessel, pericentre globular micro-steatosis, kuffe cell proliferation, diffuse hepatocyte necrosis and mononuclear infiltrate



Positive control

Section show structure of liver presented mild hepatic congestion at sinusoids and the portal vessel, pericentre globular micro-steatosis, no kuffe cell proliferation, mild hepatocyte diffuse necrosis and mononuclear infiltrate.



Treatment control-FMCuNPs

Section show structure of liver presented moderate hepatic congestion at sinusoids and the portal vessel, pericentre globular micro-steatosis, less kuffe cell proliferation, mild hepatocyte diffuse necrosis and mononuclear infiltrate.

Fig. 20: Histopathological images of the animal liver *in vivo* anticancer activity of FMCuNPs

DISCUSSION

Cancer is one of the principal causes of global morbidity and mortality. Amongst the non-infectious diseases, cancer holds the second position just after cardiovascular disease in terms of the leading cause of worldwide death. One in eight people dies due to cancer globally. The death rate due to cancer is even more than the cumulative death rate of AIDS, tuberculosis, and malaria together.

Thus globally, scientists are involved in relentless research in order to overpower cancer in the constant battle through the development in cures and preventative therapies. Cancer is typically characterized by the continual proliferation of cells in an uncontrolled manner with concomitant formation of tumour mass. In the malignant condition, few cells from the primary tumour migrate to a distant loci and form secondary cancer. Chemotherapy, radiotherapy and chemically derived drugs are most popular anticancer treatment. But unfortunately, this therapeutic measure suffers from undesirable side effects issues. Thus, a continuous hunt is going on globally to establish alternative treatments and therapies against cancer.

From ancient time, herbal medicines are considered as a very effective therapeutic approach in the Asian sub-continent. Many literature reports are also there explaining the therapeutic potential of plant-based products in the anti-cancer treatment. Quercetin is also reported to be effective against cancer [43].

Moreover, to enhance the efficacy, bioavailability, dose-response, targeting ability herbal medicines are often administered in the form of nanoparticles. In this manuscript, we have reported the green synthesis schemes of Cu-based nano particle from Quercetin isolated from aqueous extract of *Thespesia populnea*. Next, through UV-Visible Spectroscopy, FT-IR, Atomic Absorption Spectroscopy and SEM, EDAX, XRD, Zeta Potential, Particle Size Analysis we have confirmed the synthesis of the nanoparticle. Pharmacological evaluation of Quercetin-mediated copper nanoparticles confirms its anti-oxidant, anti-cancer activity.

Comparative analysis reveals that copper nanoparticles of quercetin is a better anti-oxidant and anti-cancer agent than isolated free Quercetin as confirmed by the IC₅₀ values. Furthermore, the present investigation was carried out to evaluate the anti-tumour activity of FMCuNPs in DLA tumour-bearing mice. The FMCuNPs significantly inhibited the tumour volume, packed cell volume, tumour (viable) cell count and reverse the haematological parameters to more or less normal levels. Treatment with FMCuNPs elicited the Haemoglobin (Hb) content and RBC with concomitant downregulation of WBC counts more or less to normal levels significantly.

Finally, the extension of the lifespan of animals confirms the efficacy of the anti-cancer potential of the CuNPs [19]. Usually, in cancer chemotherapy, myelosuppression and anaemia are the associated major problems [20, 21]. The anaemia encountered in tumour-bearing mice is mainly due to reduction in RBC or Haemoglobin percentage [22]. But here, we have reported that FMCuNPs possess a protective action on the haemopoietic system apart from being a potent anti-cancer agent. Moreover, it is reported that the presence of tumour in the human body or in experimental animals affect several metabolic functions of the liver. The elevated level of total cholesterol, TG, AST, ALT, ALP in serum of tumour inoculated animals indicated liver damage and loss of functional integrity of cell membrane. In the present study also, the biochemical estimation of DLA inoculated animals exhibited marked changes indicating the toxic effect of the tumour. On the contrary, the FMCuNPs induced reversal of these biochemical parameters confirms its overall anti-cancerous and hepatoprotective activity.

ACKNOWLEDGEMENT

I thank all the following individuals for their expertise and assistance throughout all aspects of our study and for their help in writing the manuscript.

Dr. D Stephen, M. Sc., Ph. D., Department of Botany, American College, Madurai for plant authentication. Dr. N. Chidambaranathan, M. Pharm., Ph. D., Department of Pharmacology, K M College of Pharmacy, Uthangudi, Madurai for *In vivo* Anti-cancer activity. Dr. S Lakshmana Prabu, M. Pharm., Ph. D., and Mr. Selvakumar, Anna University, Trichy for Particle size and Zeta potential analysis. Dr. Saravanan, Director, Instrumentation Centre, Ayya Nadar Janaki Ammal College, Sivakasi for Atomic Absorption Spectroscopy. Mr. M. Muthu, Department Of Chemistry, Madurai Kamaraj University, Madurai for NMR analysis. MR. V Krishna Prabhu, Technician, International Research Centre, Mr. Selvakumar, Kalasalingam Academy of Research and Education, Krishnakoil for FT-IR, XRD, SEM analysis. Dr. P Arulselvan, M. Sc., Ph. D., Managing Director, Scigen Research and Innovation Private Limited, Thanjavur for *In vitro* Anti-cancer activity.

CONCLUSION

Naturally, charged copper ion itself possesses a mild anti-cancer agent besides having a considerable toxic side effect. Conversion of charged species to the neutral copper or its nanoparticles is reported to augment its activity with minimising the side effects. The reduction of charged Copper ion to neutral form by chemical method involves the use of several chemical agents and also is associated with side reaction leading to the production of toxic side products. But natural product mediated reduction process of Copper ion resulting in the formation of neutral Copper atom or Copper nanoparticles can avoid the formation of undesired bi-products. In this study isolated flavonoid (natural product) used to reduce and stabilize the Copper Sulphate into Copper nanoparticles. It is environmental friendly and nontoxic method for synthesis of copper nanoparticles. In future development of Copper nanoparticles, green chemistry based synthesis is suitable for non toxic formulation and cancer target delivery.

FUNDING

Nil

AUTHORS CONTRIBUTIONS

All the authors have contributed equally.

CONFLICT OF INTERESTS

Declared none

REFERENCES

1. Appenzeller T. The man who dared to think small. *Science*. 1991;254(5036):1300. doi: 10.1126/science.254.5036.1300. PMID 17773595.
2. Murray CB, Kagan CR, Bawendi MG. Synthesis and characterization of monodisperse nanocrystals and close-packed nanocrystal assemblies. *Annu Rev Mater Sci*. 2000;30(1):545-610. doi: 10.1146/annurev.matsci.30.1.545.
3. Mazzola L. Commercializing nanotechnology. *Nat Biotechnol*. 2003;21(10):1137-43. doi: 10.1038/nbt1003-1137, PMID 14520392.
4. Paull R, Wolfe J, Hebert P, Sinkula M. Investing in nanotechnology. *Nat Biotechnol*. 2003;21(10):1144-7. doi: 10.1038/nbt1003-1144, PMID 14520393.

5. Taton TA. Nanostructures as tailored biological probes. Trends Biotechnol. 2002;20(7):277-9. doi: 10.1016/s0167-7799(02)01973-x, PMID 12062965.
6. Whitesides GM. The 'right' size in nanobiotechnology. Nat Biotechnol. 2003;21(10):1161-5. doi: 10.1038/nbt872, PMID 14520400.
7. Govil JN. Current concepts of multidiscipline approach to the medicinal plants govil n. glimpses in plant research. Part J. 1998;XII:244.
8. Chandran SP, Chaudhary M, Pasricha R, Ahmad A, Sastry M. Synthesis of gold Nano triangles and silver nanoparticles using Aloe vera plant extract. Biotechnol Prog. 2006;22(2):577-83. doi: 10.1021/bp0501423, PMID 16599579.
9. Allen JM, Xu J, Blahove M, Canonico-May SA, Santaloci TJ, Braselton ME, Stone JW. Synthesis of less toxic gold Nano rods by using dodecyl ethyl dimethylammonium bromide as an alternative growth-directing surfactant. J Colloid Interface Sci. 2017;505:1172-6. doi: 10.1016/j.jcis.2017.06.101, PMID 28715861.
10. Biao L, Tan S, Wang Y, Guo X, Fu Y, Xu F, Zu Y, Liu Z. Synthesis, characterization and antibacterial study on the chitosan-functionalized Ag nanoparticles. Mater Sci Eng C Mater Biol Appl. 2017;76:73-80. doi: 10.1016/j.msec.2017.02.154, PMID 28482584.
11. Sathishkumar P, Preethi J, Vijayan R, Mohd Yusoff AR, Ameen F, Suresh S, Balagurunathan R, Palvannan T. Anti-acne, anti-dandruff and anti-breast cancer efficacy of green synthesized silver nanoparticles using coriandrum sativum leaf extract. J Photochem Photobiol B. 2016;163:69-76. doi: 10.1016/j.jphotobiol.2016.08.005, PMID 27541567.
12. Venil CK, Sathishkumar P, Malathi M, Usha R, Jayakumar R, Yusoff ARM, Ahmad WA. Synthesis of flexirubin-mediated silver nanoparticles using *Chryseobacterium artocarpi* CECT 8497 and investigation of its anticancer activity. Mater Sci Eng C Mater Biol Appl. 2016;59:228-34. doi: 10.1016/j.msec.2015.10.019, PMID 26652368.
13. Kuppusamy P, Yusoff MM, Maniam GP, Govindan N. Biosynthesis of metallic nanoparticles using plant derivatives and their new avenues in pharmacological applications- An updated report. Saudi Pharm J. 2016;24(4):473-84. doi: 10.1016/j.jsps.2014.11.013, PMID 27330378.
14. Rehana D, Mahendiran D, Kumar RS, Rahiman AK. *In vitro* antioxidant and antidiabetic activities of zinc oxide nanoparticles synthesized using different plant extracts. Bioprocess Biosyst Eng. 2017;40(6):943-57. doi: 10.1007/s00449-017-1758-2, PMID 28361361.
15. Reddy NJ, Nagoori Vali DN, Rani M, Rani SS. Evaluation of antioxidant, antibacterial and cytotoxic effects of green synthesized silver nanoparticles by Piper longum fruit. Mater Sci Eng C Mater Biol Appl. 2014;34:115-22. doi: 10.1016/j.msec.2013.08.039, PMID 24268240.
16. Ahmad B, Hafeez N, Bashir S, Rauf A, Mujeeb-Ur-Rehman M. Phytosynthesized gold nanoparticles and their biomedical applications. Biomed Pharmacother. 2017;89:414-25. doi: 10.1016/j.biopha.2017.02.058, PMID 28249242.
17. Ovais M, Raza A, Naz S, Islam NU, Khalil AT, Ali S, Khan MA, Shinwari ZK. Current state and prospects of the phytosynthesized colloidal gold nanoparticles and their applications in cancer theranostics. Appl Microbiol Biotechnol. 2017;101(9):3551-65. doi: 10.1007/s00253-017-8250-4, PMID 28382454.
18. Jayaprakash N, Vijaya JJ, Kaviyarasu K, Kombaiha K, Kennedy LJ, Ramalingam RJ, Munusamy MA, Al-Lohedan HA. Green synthesis of Ag nanoparticles using Tamarind fruit extract for the antibacterial studies. J Photochem Photobiol B. 2017;169:178-85. doi: 10.1016/j.jphotobiol.2017.03.013, PMID 28347958.
19. Khodadadi B, Bordbar M, Nasrollahzadeh M. Green synthesis of Pd nanoparticles at apricot kernel shell substrate using *Salvia hydrangea* extract: catalytic activity for reduction of organic dyes. J Colloid Interface Sci. 2017;490:1-10. doi: 10.1016/j.jcis.2016.11.032, PMID 27870949.
20. Sathishkumar P, Vennila K, Jayakumar R, Yusoff AR, Hadibarata T, Palvannan T. Phyto-synthesis of silver nanoparticles using *Alternanthera tenella* leaf extract: an effective inhibitor for the migration of human breast adenocarcinoma (MCF-7) cells. Bioprocess Biosyst Eng. 2016;39(4):651-9. doi: 10.1007/s00449-016-1546-4, PMID 26801668.
21. Heymach J, Krilov L, Alberg A, Baxter N, Chang SM, Corcoran RB, Dale W, DeMichele A, Magid Diefenbach CSM, Dreicer R, Epstein AS, Gillison ML, Graham DL, Jones J, Ko AH, Lopez AM, Maki RG, Rodriguez-Galindo C, Schilsky RL, Szol M, Westin SN, Burstein H. Clinical cancer advances 2018: annual report on progress against cancer from the American Society of Clinical Oncology. J Clin Oncol. 2018;36(10):1020-44. doi: 10.1200/JCO.2017.77.0446, PMID 29380678.
22. Gabriel J, Chapter I. What is cancer? In: Gabriel J. The Biology of Cancer. 2nd ed. John Wiley & Sons Ltd; 2007. p. 3-9.
23. Singh DK, Lippman SM. Cancer chemoprevention. Part 1: Retinoids and carotenoids and other classic antioxidants. Oncology (Williston Park). 1998;12(11):1643-53, 1657. PMID 9834941.
24. Hussain M, Raja NI, Iqbal M, Aslam S. Applications of plant flavonoids in the green synthesis of colloidal silver nanoparticles and impacts on human health. Iran J Sci Technol Trans Sci. 2019;43(3):1381-92. doi: 10.1007/s40995-017-0431-6.
25. Tagirova MA, Vasina SM. Study an application possibility of the flavonoids for the synthesis of copper nanoparticles. Int J Eng Sci Res Technol. 2015;4(4):78-81.
26. Radhakrishnan K, Rettinaraja T, Mohan A, Jainulabideen SS. Synthesis of silver nanoparticles using flavonoid: apigenin and its antibacterial effect. EJPMPR. 2017;4(1):422-6.
27. Dhas NA, Raj CP, Gedanken A. Synthesis, characterization, and properties of metallic copper nanoparticles. Chem Mater. 1998;10(5):1446-52. doi: 10.1021/cm9708269.
28. Joshi SS, Patil SF, Iyer V, Mahumuni S. Radiation induced synthesis and characterization of copper nanoparticles. Nanostruct Mater. 1998;10(7):1135-44. doi: 10.1016/S0965-9773(98)00153-6.
29. Jana NR, Wang ZL, Sau TK, Pal T. Seed-mediated growth method to prepare cubic copper Nano particles. Curr Sci. 2000;79:1367-70.
30. Choi H, Park SH. Seedless growth of free-standing copper nanowires by chemical vapor deposition. J Am Chem Soc. 2004;126(20):6248-9. doi: 10.1021/ja049217+, PMID 15149219.
31. Guo Z, Liang X, Pereira T, Scaffaro R, Thomas Hahn HT. CuO nanoparticle filled vinyl-ester resin nanocomposites: fabrication, characterization and property analysis. Compos Sci Technol. 2007;67(10):2036-44. doi: 10.1016/j.compscitech.2006.11.017.
32. Gfeller D, Grosdidier A, Wirth M, Daina A, Michielin O, Zoete V. Swiss target prediction: a web server for target prediction of bioactive small molecules. Nucleic Acids Res. 2014;42(Web Server issue):W32-8. doi: 10.1093/nar/gku293, PMID 24792161.
33. Rana MG, Katbamna RV, Padhya AA, Dudhrejiya AD, Jivani NP, Sheth NR. *In vitro* anti-oxidant and free radical scavenging studies of alcoholic extract of *Medicago sativa* L. Rom. J Biol Plant Biol. 1996;55(1):15-22.
34. Pise NM, Jena KB, Maharana D, Sabale AB, Jagtap TG. Free radical scavenging, reducing power and biochemical composition of porphyra species. J Algal Biomass Utiln. 2010;1(2):60-73.
35. Gupta M, Mazumder UK, Kumar RS, Sivakumar T, Vamsi MLM. Antitumor activity and antioxidant status of *Caesalpinia bonducella* against Ehrlich ascites carcinoma in Swiss albino mice. J Pharmacol Sci. 2004;94(2):177-84. doi: 10.1254/jphs.94.177, PMID 14978356.
36. Jaya Seema D, Saifullah B, Selvanayagam M, Gothai S, Hussein M, Subbiah S, Mohd Esa N, Arulselvan P. Designing of the anticancer nanocomposite with sustained release properties by using graphene oxide nanocarrier with phenethyl isothiocyanate as anticancer agent. Pharmaceutics. 2018;10(3):109. doi: 10.3390/pharmaceutics10030109.
37. Christina AJ, Joseph DG, Packialakshmi M, Kothai R, Robert SJ, Chidambaranathan N, Ramasamy M. Anticarcinogenic activity of *withania somnifera* dunal against dalton's ascitic lymphoma. J Ethnopharmacol. 2004;93(2-3):359-61. doi: 10.1016/j.jep.2004.04.004, PMID 15234777.
38. Unnikrishnan MC, Kuttan R. Tumour reducing and anticarcinogenic activity of selected spices. Cancer Lett. 1990;51(1):85-9. doi: 10.1016/0304-3835(90)90235-P.

39. Agarwal RC, Rachana Jain R, Wasim Raju W, Ovais M. Anti carcinogenic effects of solanum lycopersicum fruit extract on swiss albino and C57B1 mice. *Asian Pacific J Cancer Prev.* 2009;10:379-82.
40. Bezerra DP, Castro FO, Alves APNN, DPessoa C, Moraes MO, Silveriira ER, Lima MAS, Elmiro FJM, Costa Lotufo LV. *In vivo* growth-inhibition of sarcoma 180 by pipartine and piperine, two alkaloid amides from Piper. *Brazilian Journal of Medical and Biological Research.* 2006;39(6):801-7. doi: 10.1590/s0100-879x2006000600014, PMID 16751987.
41. Chitra V, Sharma S, Kayande N. Evaluation of anticancer activity of vitex negundo study in experimental animals: *In vitro* and *in vivo* study. *International Journal of PharmTech Research.* 2009;1(4):1485-9.
42. Dongre SH, Badami S, Natesan S, H RC. Antitumor activity of the methanol extract of hypericum hookerianum stem against ehrlich ascites carcinoma in swiss albino mice. *J Pharmacol Sci.* 2007;103(4):354-9. doi: 10.1254/jphs.FP0061088.
43. Jeong JH, An JY, Kwon YT, Rhee JG, Lee YJ. Effects of low dose quercetin: cancer cell-specific inhibition of cell cycle progression. *J Cell Biochem.* 2009;106(1):73-82. doi: 10.1002/jcb.21977, PMID 19009557.